JPPIPA 12(2) (2026)

Jurnal Penelitian Pendidikan IPA

http://jppipa.unram.ac.id/index.php/jppipa/index

Development of an Empirical Rainfall Estimation Model Using Himawari-8 Infrared Satellite Data in the Lombok River Basin

Achmad Rivani[1*], Ery Setiawan[1], Atas Pracoyo[1]

[1] Department of Civil Engineering, Universitas Mataram, Mataram, Indonesia.

Received: January 29, 2026
Revised: February 16, 2026
Accepted: March 19, 2026
Published: March 20, 2026

Corresponding Author:
Achmad Rivani
achmadrivani83@gmail.com

DOI: 10.29303/jppipa.v12i2.14449

Abstract: Flooding is a recurrent hydrometeorological hazard that occurs when rainfall intensity exceeds river channel capacity within a watershed. In the Lombok River Basin, limited rain-gauge density hampers the detection of localized high-intensity rainfall that can trigger flood events. This study develops a satellite-based rainfall estimation model using Himawari-8 infrared Cloud Top Temperature (CTT) integrated with surface atmospheric parameters, including relative humidity (RH), zonal and meridional wind components (u and v), and surface air pressure (P). Hourly rainfall observations from 15 rain gauges were used for site-specific calibration during two major flood events (6 December 2021 and 17 June 2022). A local nonlinear exponential regression model was fitted for each station using the Non-Linear Least Squares (NLLS) method, and model performance was evaluated using R^2, Nash–Sutcliffe Efficiency (NSE), RMSE, and RSR. Results indicate that thermodynamic predictors, particularly CTT and RH, provide the strongest empirical relationships with rainfall variability, while wind components contribute weaker at the statistical level. Overall performance varied spatially across stations, reflecting local terrain and microclimate effects. The proposed framework supports improved rainfall characterization in tropical island basins and can be adapted to other regions with appropriate local calibration.

Keywords: Cloud top temperature; Flooding; Himawari-8; Lombok river basin; Nonlinear regression; Rainfall estimation

Introduction

Flooding is a recurrent hydrometeorological disaster triggered primarily by excessive rainfall that exceeds the discharge capacity of river channels within a watershed. Such events can cause significant damage to lives and property, particularly in catchments lacking adequate flood monitoring and management systems (Huang & Chen, 2024). In highly localized rainfall regimes, such as those commonly observed in tropical and monsoonal regions, flood occurrence is further complicated by interactions between intense rainfall, upstream inflow, and downstream boundary conditions (Meliani et al., 2025). These combined factors increase flood risk beyond what would be expected from rainfall intensity alone, highlighting the importance of accurate rainfall monitoring and short-term forecasting in watershed management.

In hydrology, a watershed constitutes the primary hydrological unit where precipitation, surface runoff, subsurface flow, and groundwater processes interact across spatial and temporal scales (Yu & Duffy, 2018), thereby serving as the fundamental basis for hydrological analysis and water resources management. Therefore, reliable representation of rainfall variability in both space and time is fundamental for hydrological modeling and flood risk assessment at the watershed scale.

Rainfall data observed by rain gauges is usually taken as a key input for hydrological analysis. However, due to the thin distribution along with a small number of rain gauges fails to represent actual spatial rainfall variation. Especially for island and complex terrain

How to Cite:
Rivani, A., Setiawan, E., & Pracoyo, A. (2026). Development of an Empirical Rainfall Estimation Model Using Himawari-8 Infrared Satellite Data in the Lombok River Basin. *Jurnal Penelitian Pendidikan IPA*, *12*(2), 752-763. https://doi.org/10.29303/jppipa.v12i2.14449

region (Vladu, 2006). Estimation of the rainfall amount and hydrologic response of rivers may become inconsistent under such a situation, leading to less confidence in flood discharge analysis.

Rainfall observations from ground-based rain gauges are traditionally used as primary inputs for hydrological analysis and flood modeling. However, limited station density and uneven spatial distribution often fail to adequately represent the true spatial variability of rainfall, particularly in mountainous and complex terrain environments (Ciach & Krajewski, 1999; Buytaert et al., 2006). Sparse rain gauge networks may lead to significant sampling errors in areal rainfall estimation and may not effectively capture localized convective events (Habib et al., 2001; Ochoa-Rodríguez et al., 2015). In tropical and island regions, rainfall variability is further influenced by orographic effects and localized atmospheric processes, increasing measurement uncertainty (Kidd & Levizzani, 2011). Consequently, uncertainties in rainfall inputs can propagate into hydrological simulations, resulting in inconsistent runoff estimation and reduced reliability of flood discharge analysis (Bitew & Gebremichael, 2011; McMillan et al., 2012).

To address the spatial limitations of point-based rainfall observations, satellite remote sensing provides a complementary source of spatially continuous rainfall information (Kidd & Huffman, 2011; Levizzani & Cattani, 2019). The Himawari-8 geostationary satellite offers high-temporal-resolution infrared observations of Cloud Top Temperature (CTT), which are widely used to detect deep convective systems associated with heavy rainfall (Bessho et al., 2016; Scofield & Kuligowski, 2003). However, the relationship between CTT and surface rainfall is inherently nonlinear, as rainfall intensity depends not only on cloud-top temperature but also on thermodynamic conditions and atmospheric dynamics within the vertical column (Houze, 2014; Vicente et al., 1998). Deep convective clouds are generally characterized by low CTT values, yet surface rainfall is further modulated by moisture availability, atmospheric stability, and wind-driven moisture transport. Therefore, incorporating additional atmospheric parameters such as relative humidity, surface pressure, and wind components can enhance the accuracy of infrared-based rainfall retrieval, particularly in tropical island environments where convective processes are highly localized (Kidd & Levizzani, 2011; Tapiador et al., 2012).

There have been numerous studies on satellite-based rainfall estimation at global and regional scales (Ayasha, 2020; Kidd & Huffman, 2011). However, many of these approaches rely on generalized parameterizations that may not adequately represent localized atmospheric–rainfall relationships in small, topographically complex basins. In tropical island environments such as the Lombok River Basin, convective processes and orographic influences can vary significantly over short distances, requiring localized calibration. Addressing this gap, the present study develops a site-specific nonlinear rainfall estimation model by establishing empirical relationships between Himawari-8 Cloud Top Temperature (CTT), selected atmospheric parameters, and observed rainfall data within the Lombok River Basin.

Method

This study was conducted in the Lombok River Basin (Figure 1), West Nusa Tenggara Province, Indonesia, a tropical island environment characterized by complex atmospheric dynamics and localized convective rainfall influenced by orographic effects. Tropical island regions are known for strong spatial rainfall variability due to interactions between large-scale circulation, local convection, and topography (Houze, 2014; Qian, 2008). The basin is also characterized by a relatively sparse rainfall observation network, which may limit accurate representation of high-intensity rainfall events.

For the development and calibration of the rainfall estimation model, continuous hourly rainfall data from 15 Automatic Weather Stations (AWS/ARR) distributed across the basin were used. Two significant flood events—6 December 2021 and 17 June 2022—were selected as representative cases for model calibration and validation. Event-based modeling is commonly adopted in hydrological studies to evaluate model stability under extreme rainfall conditions and peak discharge responses (Moriasi et al., 2007; McMillan et al., 2012).

In the Indonesian context, rainfall variability is strongly influenced by the interaction between monsoonal circulation, the Madden–Julian Oscillation (MJO), and complex island topography, which often leads to localized extreme rainfall events (Aldrian & Susanto, 2003; Hidayat & Kizu, 2010). Studies in various Indonesian watersheds have highlighted that limited rain gauge density in mountainous and island regions can reduce the reliability of flood monitoring and hydrological simulations, particularly during short-duration high-intensity storms (Hermawan et al., 2019). Given Lombok's steep terrain and maritime location, these atmospheric and topographic interactions are expected to contribute to significant spatial rainfall heterogeneity, reinforcing the need for improved rainfall estimation approaches.

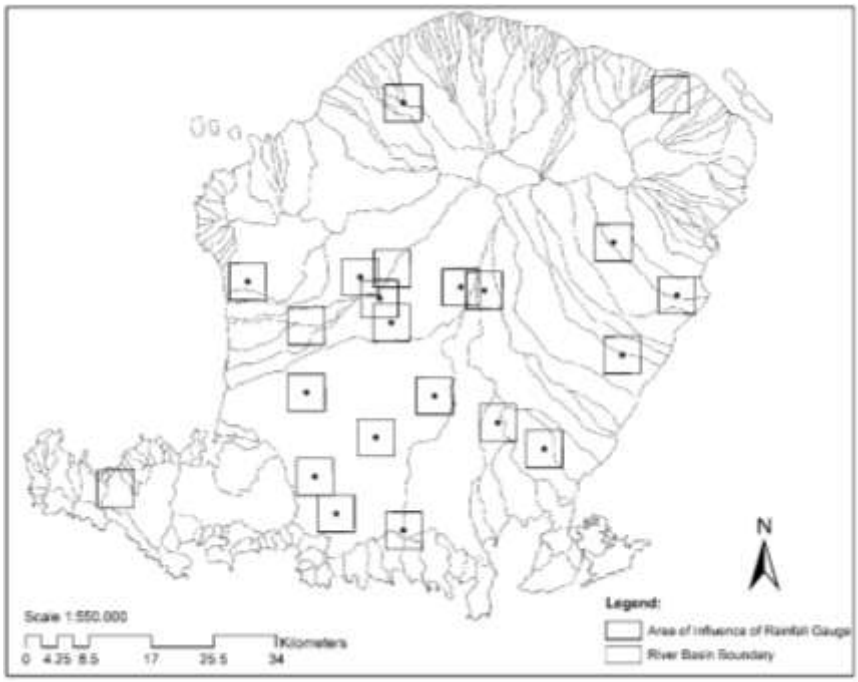

Figure 1. Lombok river basin

Data Types

This study utilized both spatial and non-spatial datasets to develop and validate the satellite-based rainfall estimation model in the Lombok River Basin. The datasets consisted of: Hourly rainfall observations were collected from all rain gauge stations (AWS/ARR and manual) distributed across the Lombok River Basin (WS Lombok); Satellite weather data (Himawari-8 Infrared Enhanced imagery to derive Cloud Top Temperature in 10-min time resolution; Atmospheric parameter datasets such as relative humidity (RH), surface air pressure, wind speed, and wind direction that reflect the behavior of atmospheric during rainfall events; and Data from the flood event to set parameters of analysis, i.e., December 6 in 2021 and June 17 in 2022.

Data Collection Method

Rainfall was registered with all functioning rain gauges in the Lombok River Basin and passed through quality control to ensure temporal consistency. The satellite data from Himawari-8 were obtained at the flood periods and processed to get CTT values.

For each rain gauge, a 25 km² Area of Interest (AOI) was defined around the station coordinates based on spatial representativeness criteria for small island environments (Linsley et al., 1986). CTT and atmospheric parameters were averaged within this AOI to reduce pixel-level noise and mitigate spatial mismatch between satellite-derived cloud-top observations and point-based rainfall measurements, including cloud displacement and parallax effects inherent to geostationary infrared imagery. This approach provides a neighborhood-scale atmospheric representation rather than relying on a single pixel. However, such averaging may partially smooth localized convective signals, particularly in complex mountainous terrain, potentially affecting model sensitivity at finer spatial scales.

Wind speed and direction were transformed into zonal (u) and meridional (v) components following standard meteorological convention, in which wind direction represents the direction from which the wind originates (Brattich et al., 2020). The transformation was computed as:

$$u = -Vsin(\theta) \quad (1)$$

$$v = -Vcos(\theta) \quad (2)$$

Where V is wind speed and θ is wind direction in degrees measured clockwise from true north. In this convention, positive $u$values indicate eastward flow and positive $v$values indicate northward flow. The negative signs account for the meteorological definition of wind direction as the direction from which the wind blows.

Data Analysis

The data were analyzed using a site-specific nonlinear regression approach. A separate regression model was developed for each rain gauge to estimate local rainfall based on satellite-derived and atmospheric predictors. The model was formulated as a multivariate exponential function incorporating normalized Cloud

Top Temperature (CTT), relative humidity (RH), zonal and meridional wind components (u and v), and surface air pressure (P) as explanatory variables. The general form of the model is express as:

$$R = a * \exp\left(b * T_{norm} + c * RH_{norm} + d * u_{norm} + e * v_{norm} + f * P\_norm\right) \quad (3)$$

Where:

R	=	predicted rainfall (mm);
a, b, c, d, e, f	=	calibrated parameters;
T_norm	=	normalized cloud top temperature;
RH_norm	=	normalized relative humidity;
u_norm, v_norm	=	normalized eastward and northward wind components;
P_norm	=	normalized air pressure

Model parameters were estimated using the Non-Linear Least Squares (NLLS) method, which minimizes the sum of squared residuals between observed and predicted rainfall. The model was calibrated and validated using cross-validation between the two selected flood events to evaluate its stability. Model performance was assessed using RMSE, NSE, and RSR. The optimal model for each rain gauge was determined based on the combination of minimum error values and maximum R^2.

Model parameters were estimated using the Non-Linear Least Squares (NLLS) method, which minimizes the sum of squared residuals between observed and predicted rainfall. The model was calibrated and validated using cross-validation between the two selected flood events to evaluate its stability.

Statistical Indicator

Nash-Sutcliffe Efficiency (NSE)

The Nash-Sutcliffe Efficiency (NSE) test is used to evaluate the accuracy of the relationship between observed and modeled data. The NSE can be calculated using the following formula.

$$NSE = 1 - \frac{\sum_{i=1}^{N}(P_i - Q_i)^2}{\sum_{i=1}^{N}(P_i - P_l)^2} \quad (4)$$

Where:

R = predicted rainfall (mm);

P_i = observed data;

Q_i = estimated (modeled) data;

P_l = mean of observed data;

N = number of data points.

Table 1. Nash-Sutchliffe Efficiency (NSE) values (Moriasi et al., 2007)

NSE	Description
0.75 < NSE ≤ 1.00	Very Good
0.65 < NSE ≤ 0.75	Good
0.50 < NSE ≤ 0.65	Satisfactory
NSE ≤ 0.50	Unsatisfactory

RMSE-Observations Standard Deviation Ratio (RSR)

Root Mean Square Error (RMSE) is one of the most commonly used statistics for error index presentation (Chu & Shirmohammadi, 2004; Singh et al., 2004; Vazquez-Amábile & Engel, 2005). While it is generally agreed that a lower RMSE indicates better model performance, Singh et al. (2004) published a guideline to qualify what is considered low RMSE based on the observations standard deviation. As recommended by Singh et al. (2004), a model evaluation statistic, the RMSE-observations standard deviation ratio (RSR), was developed. RSR is straightforward since it just normalizes RMSE with the standard deviation of the observations, and therefore it provides both an error index and extra information which, as per (Legates & McCabe Jr, 1999) recommendations. RSR can be obtained by dividing RMSE by the standard deviation of measured data as expressed in equation:

$$RSR = \frac{RMSE}{STDEV} = \frac{\left[\sqrt{\sum_{i=1}^{n}(Y_i^{obs} - Y_i^{sim})^2}\right]}{\left[\sqrt{\sum_{i=1}^{n}(Y_i^{obs} - Y_i^{mean})^2}\right]} \quad (5)$$

RMSE refers the root mean square error between simulated and observed values; STDEV_obs is the standard deviation of observed data. The RSR ranges between 0, representing perfect agreement of modeled to observed values, and larger positive numbers, where lower values represent higher agreement &rob; predictive accuracy. An RSR value of ≤ 0.5 denotes very good model performance, while values > 0.7 are indicative of poor model performance (Moriasi et al., 2007; Zahrani et al., 2025).

Error index statistics can benefit from RSR as it is a normalization factor added to the calculation that enables comparison of the results to be made over different variables. Its ideal value is 0, meaning zero RMSE and a perfect simulation of the actual model. A lower RSR value indicates less error and a better fit of the model.

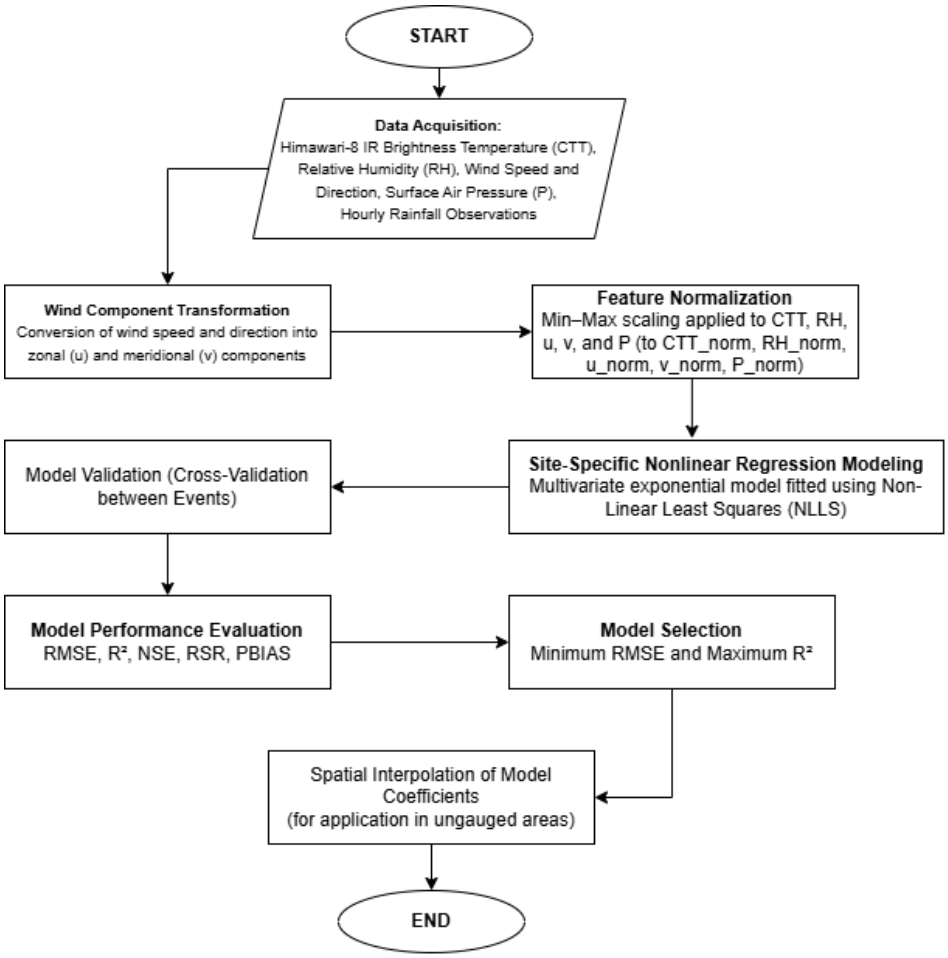

Figure 2. Flowchart of the rainfall estimation modeling framework

Result and Discussion

Processing and Retrieval of CTT (Cloud Top Temperature)

CTT data were obtained from Himawari-8 infrared-enhanced imagery released by BMKG and processed using Python-based routines to convert raster pixel information into numerical gridded datasets. RGB values were extracted with PIL/Pillow and structured into tabular format using OpenPyXL for statistical and regression analysis. Each pixel was classified according to the official BMKG color scale, representing CTT intervals from −80 to +20 °C through RGB-to-temperature mapping.

Python-based image processing frameworks are widely used in environmental and satellite data analysis due to their flexibility, reproducibility, and compatibility with open-source geospatial ecosystems (Pytroll, 2026; Tarazona et al., 2024; Meng et al., 2023; Sun et al., 2021). However, this approach relies on visually enhanced imagery rather than radiometrically calibrated Digital Number (DN) or Level-2 brightness temperature products. Radiometric calibration of Himawari-8/AHI infrared channels has been extensively documented, demonstrating that DN values represent sensor-measured radiance that can be converted into physically consistent brightness temperature using official calibration coefficients (Okuyama et al., 2018; Yu & Wu, 2016; Yu et al., 2024).

Enhanced imagery involves the application of contrast stretching and color visualization, which may introduce discretization errors and additional uncertainties into temperature conversion relative to native radiometric products. As a result, the obtained CTT values need to be treated as estimates and future studies are encouraged to implement official brightness temperature datasets to enhance physical consistency and decrease uncertainty.

The Himawari CTT map example is presented in Figure 3, based on data original image (Figure 3a) to an Excel-converted chart (Figure 3b). The extracted CTT values were charted over the rain gauge influence area boundaries to later determine average CTT.

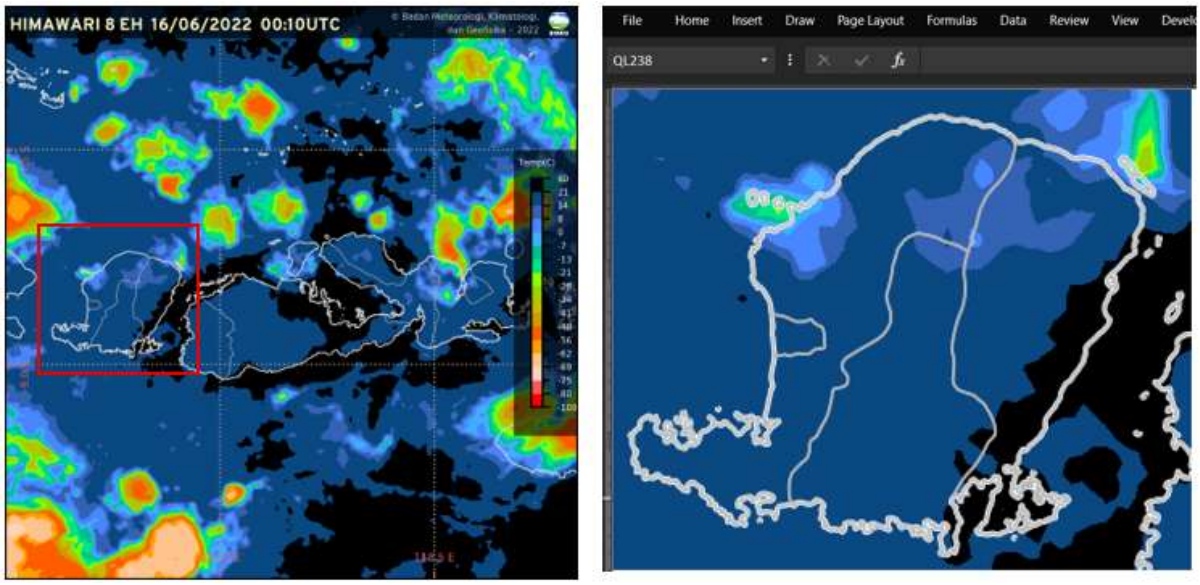

(a) (b)

Figure 3. (a) Himawari Cloud Top Temperature (CTT) Map on June 16, 2022, at 08:10 WITA; (b) Himawari Cloud Top Temperature (CTT) Map on June 16, 2022, at 08:10, central Indonesia, in Excel format

Spatial and Temporal Patterns of Cloud Top Temperature

The difference in the CTT pattern between December 2021 and June 2022 is very clear over WS Lombok. In the western-northwestern Lombok, CTT was continuously lower than that in central and eastern parts of Lombok indicating high convective activity in this portion. This CTT drop in December 2021 was strong and homogeneous throughout the network, with minimum values reaching −60 to −70 °C (as shown for Gunungsari and Sesaot stations in Figure 4), which is indicative of the appearance of a high and extensive convective cloud system. In contrast, the CTT cooling in June 2022 was local and short-lived (minimum values at around −40 to −50 °C), suggesting milder convection with limited precipitation.

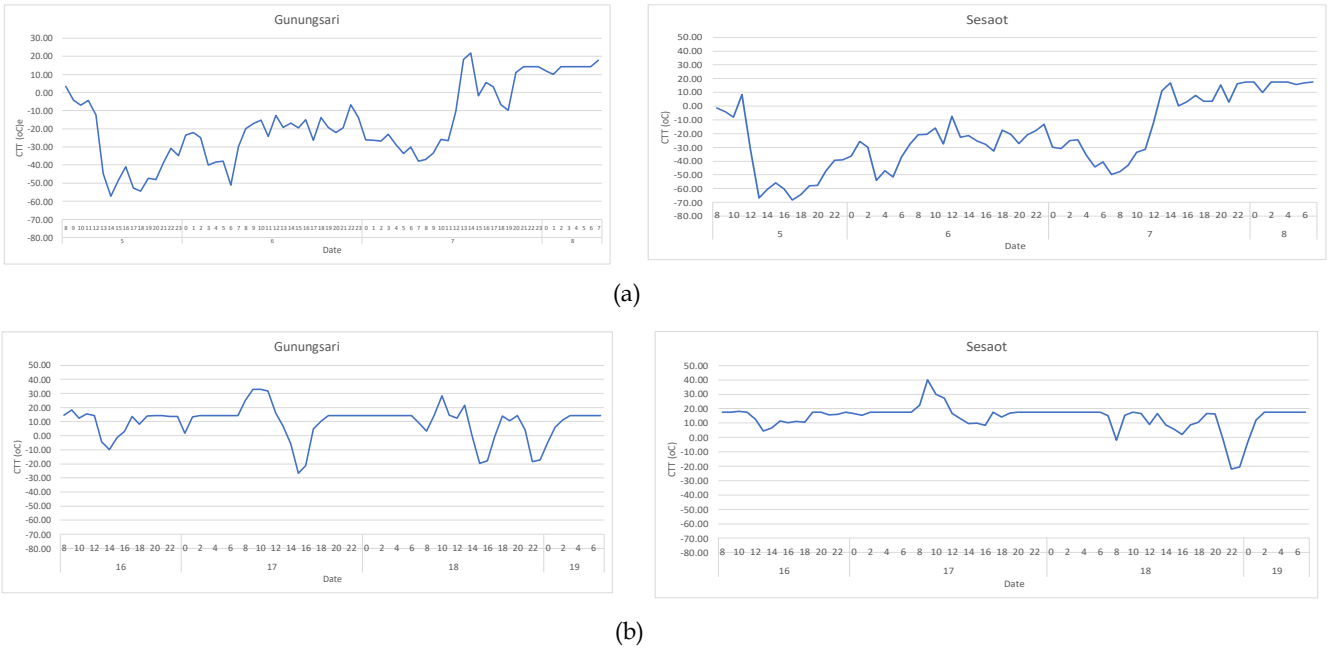

(a)

(b)

Figure 4. Temporal pattern of cloud top temperature at Gunungsari and Sesaot Stations: (a) December 2021 and (b) June 2022

Relationship between Cloud Temperature and Atmospheric Parameters

The correlation analysis between CTT and surface atmospheric parameters (T, RH, u, v, and P) in the Lombok River Basin indicates that CTT and relative humidity exhibit stronger statistical relationships with rainfall intensity compared to the wind components. As shown in Figure 5 for the Gunungsari and Sesaot stations, higher correlation values are observed for rainfall–CTT and rainfall–RH pairs, suggesting that thermodynamic variables play a significant role in explaining rainfall variability within the analyzed events.

However, this does not imply that dynamic factors are physically unimportant. In tropical island environments such as Lombok, wind-driven moisture transport and orographic lifting are essential components of rainfall formation. The relatively weaker statistical correlation of wind components (u, v) in this analysis may be influenced by differences in temporal resolution between atmospheric wind data and satellite-derived CTT, as well as the nonlinear nature of dynamic processes. Therefore, both thermodynamic and dynamic factors contribute to rainfall formation, although their statistical representation may vary depending on data resolution and event characteristics.

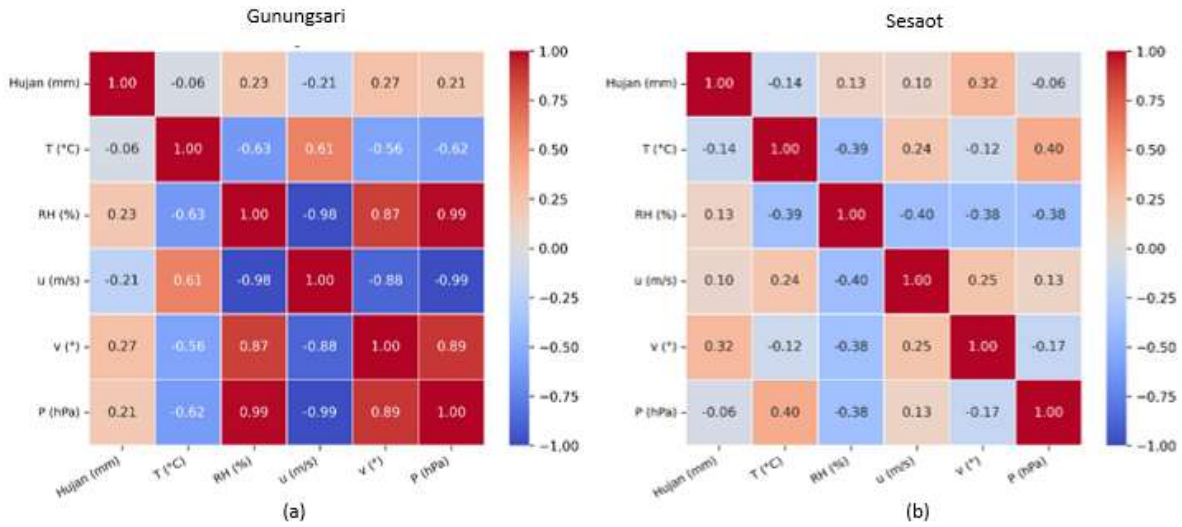

Figure 5. Rainfall correlation at Gunungsari Station (a) and Sesaot Station (b) with atmospheric parameters

Development and Validation of the Rainfall Estimation Model

The rainfall estimation model was developed using a site-specific nonlinear regression approach, in which separate models were calibrated for each rain gauge. This approach was adopted because rainfall patterns in the Lombok River Basin exhibit strong spatial variability; therefore, the relationship between atmospheric parameters and rainfall may differ across locations (Figure 6). For each station, regression coefficients were independently calibrated and evaluated. The models were then compared based on their performance metrics, and the best-performing configuration for each rain gauge was selected to minimize prediction bias (Table 1).

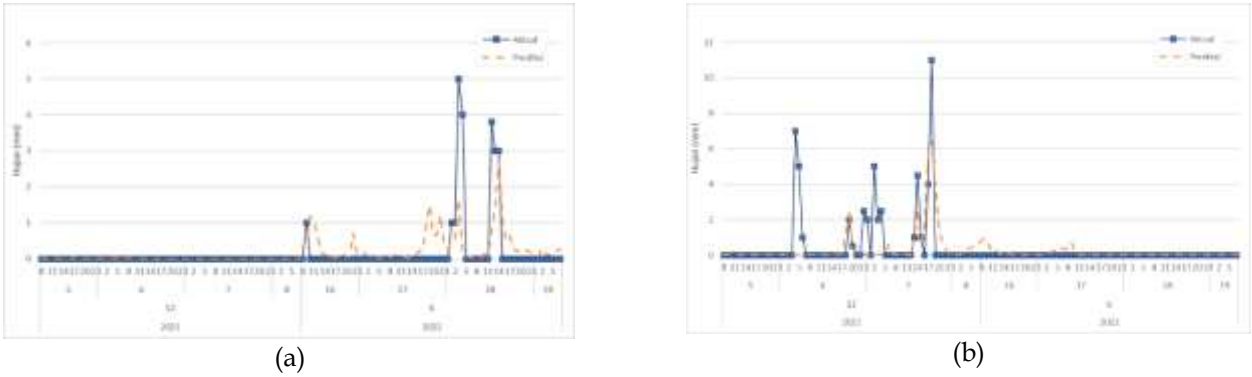

Figure 6. Comparison of actual and predicted rainfall at Gunungsari Rain Gauge (a) and Sesaot Rain Gauge (b)

Table 2. Performance of the rainfall estimation model for each rain gauge

Rain Gauge	RMSE (mm)	NSE	RSR	Model Coefficients					
				a	b (T_norm)	c (RH_norm)	d (u_norm)	e (v_norm)	f (P_norm)
Batujai	0.705	0.933	0.258	6.5 E-01	-6.6857	-8.0300	10.0000	-5.5931	-1.7001
Gunungsari	0.593	0.309	0.832	8.0 E-05	2.7012	10.0000	8.4599	-7.3752	-1.1024
Ijobalit	0.682	0.79	0.458	9.8 E-02	0.8273	-9.3239	10.0000	-10.0000	0.0053
Jurangsate	1.787	0.517	0.695	1.8 E-06	-3.9981	8.0634	10.0000	0.3335	3.0125
Kuripan	0.858	0.186	0.902	4.5 E-03	-2.2725	5.4808	3.3908	-6.6749	1.1380
Lingkok Lime	1.552	0.591	0.639	7.1 E-02	-4.2364	10.0000	1.7227	-10.0000	-6.1335
Loang Make	2.074	0.225	0.88	8.3 E-01	2.6501	10.0000	-7.0292	-10.0000	-9.5465
Mangkung	1.766	0.863	0.37	1.8 E-03	-5.8880	10.0000	7.7338	2.2763	-10.0000
Pengadang	0.602	0.253	0.864	4.9 E-04	-5.3613	1.7860	9.0986	4.8204	-2.9774
Perian	0.041	0.88	0.346	1.0 E-08	9.3831	8.7047	-2.8216	-10.0000	10.0000
Pringgabaya	0.381	0.205	0.892	3.6 E-03	-8.7554	2.9460	0.0505	10.0000	-6.8441
Santong	1.698	0.19	0.9	3.6 E-02	10.0000	0.8306	-10.0000	3.3553	-7.6228
Sapit	0.094	0.697	0.551	8.7 E-02	-6.6015	10.0000	-6.6255	-10.0000	1.3605
Sepit	1.528	0.383	0.785	1.1 E+01	-6.2005	-0.9433	3.7214	1.6837	-8.4232
Sesaot	1.094	0.352	0.805	5.3 E-06	6.0607	3.8238	7.4127	-10.0000	5.5774

Table 2 illustrates that model performance differs significantly at the rain gauge stations throughout the basin. Overall NSEs fall between 0.186 and 0.933, demonstrating high spatial variability in predictive skill. NSE > 0.75 indicates very good performance, 0.65–0.75 good, 0.50–0.65 satisfactory and < 0.50 unsatisfactory according to widely accepted criteria for evaluating hydrological models (Moriasi et al., 2007; Moriasi et al., 2015). From these cutoff points, Batujai (0.933), Ijobalit (0.79), and Mangkung (0.863) exhibit very good model performance, and stations in the unsatisfactory or satisfactory categories are also present from these parameter values. This variability is attributable to differences in local rainfall properties, topography influence and the representativeness of satellite-based predictors.

The RMSE values range from 0.041 mm (Perian) to 2.074 mm (Loang Make), highlighting variability in absolute prediction error between the stations. Good agreement between estimated and observed rainfall leads to lower RMSE values. The RSR values range from 0.258 to 0.902, where smaller RSR indicates less residual variance as compared with observed standard deviation and thus better model performance (Moriasi et al., 2007). High predictive reliability is shown by the RSR < 0.50 while a value above it, near or greater than 0.70 indicates poor performance. Classification results for HDS system validation on waiting time predictions from stations with and EAF values of some of the total data points mapped to peak hour grid were strong stability aside low accuracy as it'd be expected in comparison as well other hand predictability was noteworthy (altogether with reach channel's prediction).

Furthermore, the PBIAS values vary from −26.469 to 89.401%, indicating the occurrence of both underestimation (negative bias) and overestimation (positive bias). The relatively large positive PBIAS values at some stations point toward overestimation of rainfall intensity from satellite-based predictors under specific convective conditions, resulting in negative values that show systematic underprediction. Bias variability of this nature is a common occurrence in satellite-derived rainfall modeling, especially in the recognized geographic regions of high spatial rainfall heterogeneity and orographic effects (Hou et al., 2014; Kidd & Huffman, 2011).

The overall naive site specific nonlinear regression model performs reasonably well for several stations, especially those that comply with fairly welldefined rainfall patterns coupled with fixer predictor-response relationships. However, performance is not spatially uniform and reflects local microclimate variability and complex terrain conditions in Lombok River Basin. This result is in line with previous research indicating that the accuracy of satellite-based rainfall estimates diminishes when it comes to mountainous and coastal transitional areas due to cloud-top temperature ambiguity and vertical structure variability, respectively (Tang et al., 2023).

Interpolation of Model Coefficients

In order to transfer the local rainfall–predictor models to ungauged areas, we spatially interpolated regression coefficients (a–f) of 15 stations into basin-wide surfaces of regression coefficients (Figures 7 to 12), based on principles from hydrological regionalization (Blöschl et al., 2019). Although this retains the nonlinear model structure, uncertainty increases further from stations, particularly in highly complex terrain, and predictions in such locations should be treated with caution.

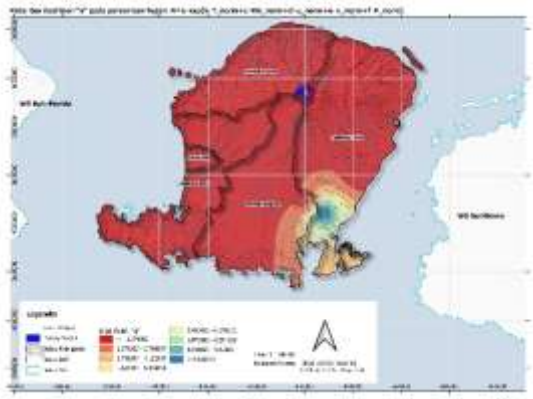

Figure 7. Interpolation of model coefficient "a"

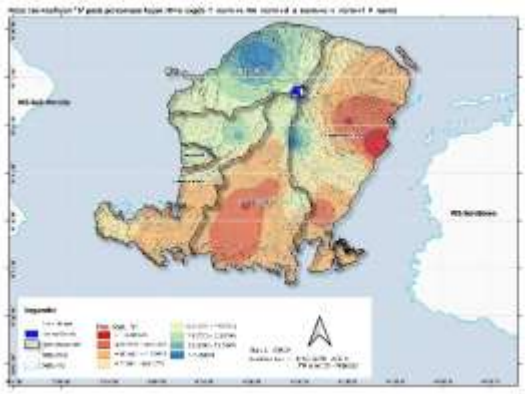

Figure 8. Interpolation of model coefficient "b"

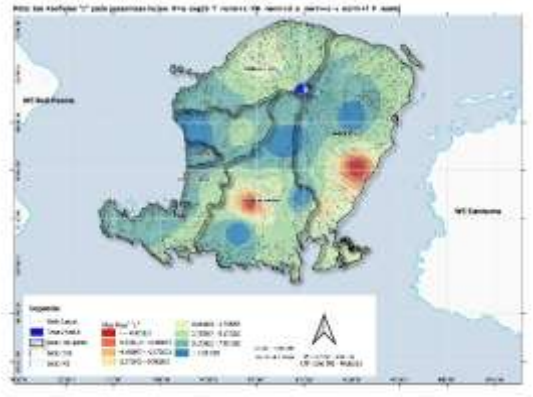

Figure 9. Interpolation of model coefficient "c"

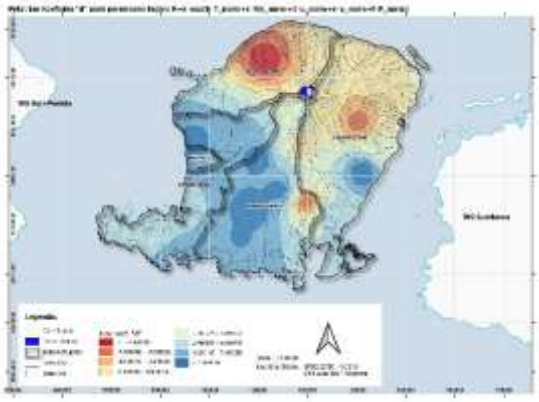

Figure 10. Interpolation of model coefficient "d"

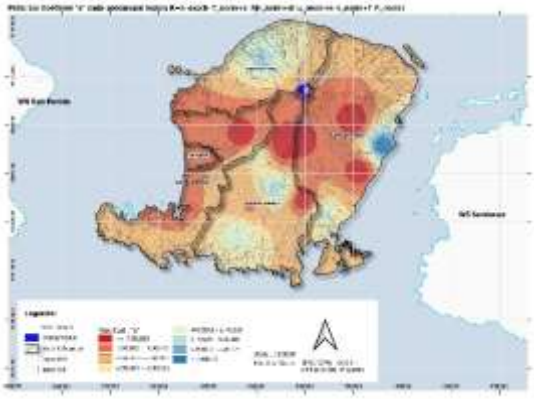

Figure 11. Interpolation of model coefficient "e"

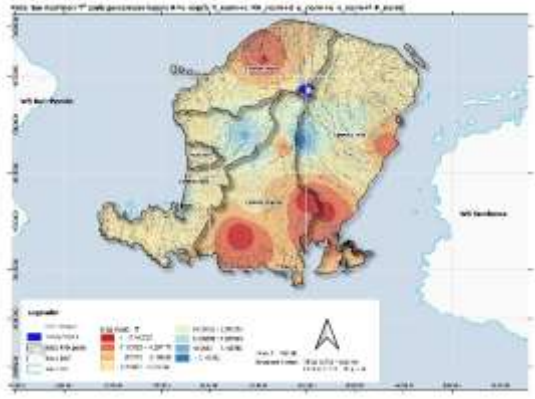

Figure 12. Interpolation of model coefficient "f"

Conclusion

This study developed a satellite-based rainfall estimation framework using Himawari-8 infrared Cloud Top Temperature (CTT) integrated with surface atmospheric parameters and calibrated individually at each rain gauge in the Lombok River Basin. The analysis revealed distinct rainfall characteristics between the December 2021 and June 2022 events, with the former exhibiting stronger and more extensive convective activity as indicated by lower CTT values. The results show that thermodynamic variables, particularly CTT and relative humidity, exhibit stronger statistical associations with rainfall variability, while dynamic factors represented by zonal and meridional wind components (u and v) contribute through moisture transport and circulation processes. The site-specific nonlinear regression approach enables localized calibration of satellite-to-rainfall relationships, improving representation of spatial variability within the Lombok River Basin. Although the model is specifically calibrated for Lombok, the methodological framework may be adapted to other regions with similar climatic characteristics, provided that local calibration

using ground observations is performed. Further validation in different geographic settings is required before broader regional application.

Acknowledgments
The authors would like to express their sincere gratitude to their academic supervisor for the guidance, valuable insights, and constructive feedback provided throughout the research process. The authors also acknowledge the Balai Besar Wilayah Sungai Nusa Tenggara I for supporting this study through the provision of hourly rainfall data. Appreciation is further extended to the Class II Meteorological Station Zainuddin Abdul Madjid for providing Himawari satellite imagery data. The authors are also grateful to colleagues for their constructive discussions, suggestions, and comments during the completion of this research.

Author Contributions
Conceptualization and methodology, data collection and analysis, writing—original draft, A.R.; writing—review and editing, supervision, E.S. and A.P. All authors have read and approved the final manuscript.

Funding
This research received no external funding and was supported by the authors' personal resources.

Conflicts of Interest
The authors declare no conflict of interest.

References

Aldrian, E., & Susanto, R. D. (2003). Identification of Three Dominant Rainfall Regions within Indonesia and Their Relationship to Sea Surface Temperature. *International Journal of Climatology*, *23*(12), 1435–1452. https://doi.org/10.1002/joc.950

Ayasha, N. (2020). A Comparison of Rainfall Estimation Using Himawari-8 Satellite Data in Different Indonesian Topographies. *International Journal of Remote Sensing and Earth Sciences*, *17*(2), 189–200. https://doi.org/10.30536/ijreses.v17i2.13815

Bessho, K., Date, K., Hayashi, M., Ikeda, A., Imai, T., Inoue, H., ... & Yoshida, R. (2016). An Introduction to Himawari-8/9—Japan's New-Generation Geostationary Meteorological Satellites. *Journal of the Meteorological Society of Japan*, *94*(2), 151–183. https://doi.org/10.2151/jmsj.2016-009

Bitew, M. M., & Gebremichael, M. (2011). Evaluation of Satellite Rainfall Products Through Hydrologic Simulation in a Fully Distributed Hydrologic Model. *Water Resources Research*, *47*(6). https://doi.org/10.1029/2010WR009917

Blöschl, G., Hall, J., Viglione, A., Perdigão, R. A. P., Parajka, J., Merz, B., Lun, D., Arheimer, B., Aronica, G. T., Bilibashi, A., Boháč, M., Bonacci, O., Borga, M., Čanjevac, I., Castellarin, A., Chirico, G. B., Claps, P., Frolova, N., Ganora, D., Gorbachova, L., … Živković, N. (2019). Changing Climate Both Increases and Decreases European River Floods. *Nature*, *573*(7772), 108–111. https://doi.org/10.1038/s41586-019-1495-6

Brattich, E., Orza, J. A. G., Cristofanelli, P., Bonasoni, P., Marinoni, A., & Tositti, L. (2020). Advection Pathways at the Mt. Cimone WMO-GAW Station: Seasonality, Trends, and Influence on Atmospheric Composition. *Atmospheric Environment*, *234*, 117513. https://doi.org/10.1016/j.atmosenv.2020.117513

Buytaert, W., Celleri, R., Willems, P., Bièvre, B. D., & Wyseure, G. (2006). Spatial and Temporal Rainfall Variability in Mountainous Areas: A Case Study from the South Ecuadorian Andes. *Journal of Hydrology*, *329*(3–4), 413–421. https://doi.org/10.1016/j.jhydrol.2006.02.031

Chu, T. W., & Shirmohammadi, A. (2004). Evaluation of the SWAT Model's Hydrology Component in the Piedmont Physiographic Region of Maryland. *Transactions of the ASAE*, *47*(4), 1057–1073. https://doi.org/10.13031/2013.16579

Ciach, G. J., & Krajewski, W. F. (1999). On the Estimation of Radar Rainfall Error Variance. *Advances in Water Resources*, *22*(6), 585–595. https://doi.org/10.1016/S0309-1708(98)00043-8

Habib, E., Krajewski, W. F., & Kruger, A. (2001). Sampling Errors of Tipping-Bucket Rain Gauge Measurements. *Journal of Hydrologic Engineering*, *6*(2), 159–166. https://doi.org/10.1061/(ASCE)1084-0699(2001)6:2(159)

Hermawan, E., Norfahmi, S. H., Suryantoro, A., Harjana, T., Trismidianto, T., Purwaningsih, A., & Azizah, S. (2019). Characteristics of Extreme Rainfall Over the Indonesian Equatorial Region Based on Madden–Julian Oscillation Index Analysis. *Journal of Physics: Conference Series*, *1373*, 012002. https://doi.org/10.1088/1742-6596/1373/1/012002

Hidayat, R., & Kizu, S. (2010). Influence of the Madden–Julian Oscillation on Indonesian Rainfall Variability in Austral Summer. *International Journal of Climatology*, *30*(12), 1816–1825. https://doi.org/10.1002/joc.2005

Hou, A. Y., Kakar, R. K., Neeck, S., Azarbarzin, A. A., Kummerow, C. D., Kojima, M., ... & Iguchi, T. (2014). The Global Precipitation Measurement Mission. *Bulletin of the American Meteorological Society*, *95*(5), 701–722. https://doi.org/10.1175/BAMS-D-13-00164.1

Houze, R. A. J. (2014). *Cloud Dynamics*. Academic Press.

Huang, Z., & Chen, Y. (2024). Impact of Rain Gauge Density on Flood Forecasting Performance: A

PBDHM's Perspective. *Water*, *17*(1), 18. https://doi.org/10.3390/w17010018

Kidd, C., & Huffman, G. (2011). Global Precipitation Measurement. *Meteorological Applications*, *18*(3), 334–353. https://doi.org/10.1002/met.284

Kidd, C., & Levizzani, V. (2011). Status of Satellite Precipitation Retrievals. *Hydrology and Earth System Sciences*, *15*(4), 1109–1116. https://doi.org/10.5194/hess-15-1109-2011

Legates, D. R., & McCabe Jr, G. J. (1999). Evaluating the Use of Goodness-of-Fit Measures in Hydrologic Model Validation. *Water Resources Research*, *35*(1), 233–241. https://doi.org/10.1029/1998WR900018

Levizzani, V., & Cattani, E. (2019). Satellite Remote Sensing of Precipitation and the Terrestrial Water Cycle in a Changing Climate. *Remote Sensing*, *11*(19), 2301. https://doi.org/10.3390/rs11192301

Linsley, R., Kohler, M., & Paulhus, J. (1986). *Hydrology for Engineers*. 3rd Edition. New York: McGraw-Hill Publications.

McMillan, H., Krueger, T., & Freer, J. (2012). Benchmarking Observational Uncertainties for Hydrology. *Hydrological Processes*, *26*(26), 4078–4111. https://doi.org/10.1002/hyp.9384

Meliani, F., Sulistyowati, R., Sapan, E. G. A., Sumargana, L., Lestari, S., Suryanta, J., Rudiastuti, A. W., Cahyaningtiyas, I. F., Pianto, T. A., Akbar, H. I., Yulianingsani, Y., Winarno, W., Priyadi, H., Cahya, D. L., Winarno, B., & Sutejo, B. (2025). The Influence of the Rainfall Extremes and Land Cover Changes on the Major Flood Events at Bekasi, West Jawa, and Its Surrounding Regions. *Resources*, *14*(11), 169. https://doi.org/10.3390/resources14110169

Meng, X-N., Xu, S-C., & Hao, M-G. (2023). Can Digital-Real Integration Promote Industrial Green Transformation: Fresh Evidence from China's Industrial Sector. *Journal of Cleaner Production*, *426*, 139116. https://doi.org/10.1016/j.jclepro.2023.139116

Moriasi, D. N., Arnold, J. G., Liew, M. W. V., Bingner, R. L., Harmel, R. D., & Veith, T. L. (2007). Model Evaluation Guidelines for Systematic Quantification of Accuracy in Watershed Simulations. *Transactions of the ASABE*, *50*(3), 885–900. https://doi.org/10.13031/2013.23153

Moriasi, D. N., Gitau, M. W., Pai, N., & Daggupati, P. (2015). Hydrologic and Water Quality Models: Performance Measures and Evaluation Criteria. *Transactions of the ASABE*, *58*(6), 1763–1785. https://doi.org/10.13031/trans.58.10715

Ochoa-Rodríguez, S., Wang, L. P., Gires, A., Pina, R. D., Reinoso-Rondinel, R., Bruni, G., ... & Veldhuis, M. C. T. (2015). Impact of Spatial and Temporal Resolution of Rainfall Inputs on Urban Hydrodynamic Modelling Outputs: A Multi-Catchment Investigation. *Journal of Hydrology*, *531*, 389–407. https://doi.org/10.1016/j.jhydrol.2015.05.035

Okuyama, A., Takahashi, M., Date, K., Hosaka, K., Murata, H., Tabata, T., & Yoshino, R. (2018). Validation of Himawari-8/AHI Radiometric Calibration Based on Two Years of in-Orbit Data. *Journal of the Meteorological Society of Japan*. https://doi.org/10.2151/jmsj.2018-033

Pytroll, P. (2026). *Satpy: Python Package for Earth-Observing Satellite Data Processing*. Retrieved from https://github.com/pytroll/satpy

Qian, J. H. (2008). Why Precipitation is Mostly Concentrated Over Islands in the Maritime Continent. *Journal of the Atmospheric Sciences*, *65*(4), 1428–1441. https://doi.org/10.1175/2007JAS2422.1

Scofield, R. A., & Kuligowski, R. J. (2003). Status and Outlook of Operational Satellite Precipitation Algorithms for Extreme-Precipitation Events. *Weather and Forecasting*, *18*(6), 1037–1051. https://doi.org/10.1175/1520-0434(2003)018%3C1037:SAOOOS%3E2.0.CO;2

Singh, J., Knapp, H. V., & Demissie, M. (2004). *Hydrologic Modeling of the Iroquois River Watershed Using HSPF and SWAT*. Illinois State Water Survey.

Sun, X., Gnanamuthu, S., Zagade, N., Wang, P., & Bright, J. M. (2021). Full Disk Real-Time Himawari-8/9 Satellite AHI Imagery from JAXA. *Journal of Renewable and Sustainable Energy*, *13*(6). https://doi.org/10.1063/5.0062477

Tang, X., Li, H., Qin, G., Huang, Y., & Qi, Y. (2023). Evaluation of Satellite-Based Precipitation Products Over Complex Topography in Mountainous Southwestern China. *Remote Sensing*, *15*(2), 473. https://doi.org/10.3390/rs15020473

Tapiador, F. J., Turk, F. J., Petersen, W., Hou, A. Y., García-Ortega, E., Machado, L. A., ... & Castro, M. D. (2012). Global Precipitation Measurement: Methods, Datasets and Applications. *Atmospheric Research*, *104*, 70–97. https://doi.org/10.1016/j.atmosres.2011.10.021

Tarazona, Y., Benitez-Paez, F., Nowosad, J., Drenkhan, F., & Timaná, M. E. (2024). Scikit-eo: A Python Package for Remote Sensing Data Analysis. *Journal of Open Source Software*, *9*(99), 6692. https://doi.org/10.21105/joss.06692

Vazquez-Amábile, G. G., & Engel, B. A. (2005). Use of SWAT to Compute Groundwater Table Depth and Streamflow. *Transactions of the ASAE*, *48*(3), 991–1003. https://doi.org/10.13031/2013.18511

Vicente, G. A., Scofield, R. A., & Menzel, W. P. (1998). The Operational GOES Infrared Rainfall Estimation Technique. *Bulletin of the American Meteorological Society*, *79*(9), 1883–1898. Retrieved from https://www.jstor.org/stable/26214869

Vladu, I. F. (2006). *Adaptation as Part of the Development Process*. Technology Sub-Programme, Adaptation, Technology and Science Programme, UNFCCC (United Nations Framework Convention on Climate Change)

Yu, F., & Wu, X. (2016). Radiometric Inter-Calibration between Himawari-8 AHI and S-NPP VIIRS for the Solar Reflective Bands. *Remote Sensing*, *8*(3), 165. https://doi.org/10.3390/rs8030165

Yu, X., & Duffy, C. J. (2018). Watershed Hydrology: Scientific Advances and Environmental Assessments. *Water*, *10*(3), 288. https://doi.org/10.3390/w10030288

Yu, Y., Renzullo, L. J., McVicar, T. R., Niel, T. G. V., Cai, D., Tian, S., & Ma, Y. (2024). Solar Zenith Angle-Based Calibration of Himawari-8 Land Surface Temperature. *Remote Sensing of Environment*, *308*, 114176. https://doi.org/10.1016/j.rse.2024.114176

Zahrani, N., Suhartanto, E., & Andawayanti, U. (2025). Assessment of Bias-Correction Methods for CHIRPS Satellite Rainfall Estimates in the Petung Watershed, Indonesia. *Jurnal Penelitian Pendidikan IPA*, *11*(12), 43–51. https://doi.org/10.29303/jppipa.v11i12.13250